Mechanochemical Reduction of Magnesium Ferrite

Vladimír Šepelák†

Institute of Geotechnics, Slovak Academy of Sciences, Watsonova 45, SK-04353 Košice, Slovakia

Marcus Menzel and Klaus Dieter Becker*

Institute of Physical and Theoretical Chemistry, Technical University of Braunschweig, Hans-Sommer-Str. 10, D-38106 Braunschweig, Germany

Frank Krumeich

Laboratory of Inorganic Chemistry, Swiss Federal Institute of Technology Zurich, Hönggerberg, CH-8093 Zurich, Switzerland

Received: January 29, 2002

The changes in magnesium ferrite, $MgFe_2O_4$, due to high-energy milling in a stainless steel vial have been investigated by Mössbauer spectroscopy, X-ray diffraction, electron microscopy, and thermal analysis. The milling process reduces the average crystallite size of $MgFe_2O_4$ to the nanometer range. Prolonged mechanical treatment leads to the chemical reduction of $MgFe_2O_4$ and to the formation of a solid solution of FeO and MgO. In addition to the solid solution, metallic iron has been found as a byproduct. The fraction of the reaction products increases with increasing milling time. The range of thermal stability of the metastable milled reduction products has been determined by studying their response to changes in temperature.

Introduction

Mechanically activated processes continue to attract considerable attention in the field of solid-state chemistry, physics, and materials science. Mechanical treatment (mechanical activation, high-energy milling) of crystalline compounds has been employed to prepare solids far from equilibrium, such as amorphous alloys, nanostructured materials, and quasicrystalline phases.[1]

Reduction processes induced by mechanical treatment represent an important class of solid-state reactions. Many examples have been reported where reduction of simple binary oxides by a more reactive metal occurs during milling.[2−10] In ball-milling experiments involving α-Fe_2O_3 in air, reduction of α-Fe_2O_3 to Fe_3O_4[11−14] and subsequently, to the $Fe_{1-x}O$ phase[15] has been observed to occur in a closed stainless steel container after prolonged milling. Depending upon the value of the adiabatic temperature of the redox reaction and milling conditions, the reaction may occur either in a steady-state manner during milling or by unstable thermal combustion of the reactants.[16] In addition to simple oxides, there have also been reports on the reduction of chlorides during high-energy milling.[17]

While the mechanically induced redox reactions involving simple binary oxides are discussed extensively in the literature, the mechanochemical reduction of higher complex oxides is treated only to a limited extent. In this context, the mechanically induced reduction of ilmenite ($FeTiO_3$) and scheelite ($CaWO_4$) may be mentioned.[18,19] To our best knowledge, the application of high-energy milling to the chemical reduction of oxide spinels has been reported in only a few papers.[4,20−26] There have been reports on the reduction of Fe_3O_4 during high-energy milling.[4,20−22] $NiFe_2O_4$ and $CuFe_2O_4$ appear to be the only ternary spinels that have been investigated.[24−26] The high-energy milling of $NiFe_2O_4$ in a steel vial using steel balls was found to induce a mechanochemical reduction process of the material leading to the formation of a disordered solid solution of FeO and NiO with wüstite structure.[24,25] Goya et al.[26] followed the phase evolution of $CuFe_2O_4$ during high-energy milling. They showed that the final product of the mechanical treatment of copper ferrite is a two-phase mixture consisting of Fe_3O_4 and a spinel solid solution ($Cu_xFe_{3-x}O_4$). This indicates that the high-energy milling of the ferrite spinel generates a complex series of solid-state transformations, including mechanochemical decomposition and reduction.

In this work, we present a detailed study of the phase evolution of $MgFe_2O_4$ during high-energy milling in a stainless steel vial. Magnesium ferrite is a soft magnetic material,[27] which finds a number of applications in heterogeneous catalysis and adsorption, in sensor and in magnetic technologies. To emphasize the site occupancy on the atomic level, $MgFe_2O_4$ may be written as $(Mg_{1-\lambda}Fe_\lambda)[Mg_\lambda Fe_{2-\lambda}]O_4$, where parentheses and square brackets denote cation sites of tetrahedral (A) and octahedral [B] coordination, respectively. λ represents the so-called degree of inversion (defined as the fraction of the (A) sites occupied by Fe^{3+} cations) characterizing the distribution of cations among the two nonequivalent sites. In recent work,[28−30] we have demonstrated that high-energy milling of $MgFe_2O_4$ in ceramic-covered vials using ceramic α-Al_2O_3 balls does not lead to chemical reduction: no other phases except the nanoscale $MgFe_2O_4$ were detected in the milled powders. It has been found, however, that these $MgFe_2O_4$ nanoparticles

* Author to whom correspondence should be addressed. Fax: +49-531-3917305. E-mail: k-d.becker@tu-bs.de.

† Present address: Institute of Physical and Theoretical Chemistry, Technical University of Braunschweig, Hans-Sommer-Str. 10, D-38106 Braunschweig, Germany. Fax: +49-531-3917305. E-mail: v.sepelak@tu-bs.de.

10.1021/jp020270z CCC: $22.00
Published on Web 06/06/2002

are structurally and magnetically disordered due to mechanically induced changes in the cation distribution and spin canting.

Experimental Section

Polycrystalline magnesium ferrite was prepared by conventional solid-state reaction (further referred to as the nonactivated material). Stoichiometric mixtures of the powdered reactants α-Fe_2O_3 and MgO (Merck, Darmstadt) were homogenized in a ball mill. The powdered mixtures were pressed into tablets under a pressure of 30 MPa in a steel die in order to obtain a high degree of compaction of the reactants. The tablets were 20 mm in diameter and 4 mm thick. They were prefired twice at 1200 K for 24 h, ground, pressed, and finally sintered at 1300 K for 24 h (all processes in air). The single-phase nature of the as-prepared samples was confirmed by X-ray diffraction (XRD) and Mössbauer spectroscopy.

The high-energy milling process (dry milling) was carried out in an AGO 2 planetary ball mill (Institute of Solid State Chemistry and Mechanochemistry, Novosibirsk) at room temperature. The nonactivated sample (10 g) was ground for various times in a closed, air-filled vial (150 cm^3 in volume) made of hardened stainless steel together with hardened stainless steel balls. The ball-to-powder weight ratio was 20:1. Milling experiments were performed in air at 750 rpm.

Mössbauer measurements were performed in transmission geometry using a microcomputer-controlled spectrometer in constant acceleration mode using a ^{57}Co/Rh γ-ray source. The velocity scale was calibrated relative to ^{57}Fe in Rh. The transmitted γ-radiation was detected by means of a proportional counter. "Recoil" spectral analysis software[31] was used for the quantitative evaluation of the Mössbauer spectra.

XRD patterns were collected using a URD 6 powder diffractometer (Seifert-FPM, Freiberg) with Cu Kα or Fe Kα radiation. XRD patterns were analyzed using the STADI P software (Stoe, Darmstadt). The JCPDS database was utilized for phase identification. An XRK-A Paar camera (Paar GmbH, Graz) was employed for in situ X-ray diffraction in the temperature range between 300 and 1100 K. Samples were heated in a flowing nitrogen atmosphere at a heating rate of 2 K min^{-1}. Typically, the partial pressure of residual oxygen in the nitrogen gas used in the present experiments was of the order of 10^{-4} atm.

The morphology of the powder and the sizes of individual crystallites were studied by means of transmission electron microscopy (TEM) (model CM30ST, Philips, Eindhoven). The particle size distribution was measured by laser radiation scattering (Laser-Particle-Sizer Analyzette 22 Granulometer, Fritsch, Idar-Oberstein). Mean particle diameters and specific surface areas were calculated from the granulometric data.

Thermoanalytical measurements were performed using a SETARAM TAG 24 thermobalance with simultaneous differential thermal analysis. Samples of 130 mg were heated in open platinum crucibles up to 1100 K at a heating rate of 10 K min^{-1} in flowing nitrogen gas.

Results and Discussion

The mechanically induced evolution of $MgFe_2O_4$ submitted to the high-energy milling process has been followed by ^{57}Fe Mössbauer spectroscopy. Figure 1 shows the Mössbauer spectrum of nonactivated $MgFe_2O_4$ taken at room temperature in an applied magnetic field of 5.5 T. The subspectra of both (A)- and [B]-site ferric ions are indicated. The Mössbauer spectrum of nonactivated $MgFe_2O_4$ taken in zero applied magnetic field, Figure 2a, exhibits a considerable overlap of the (A) and [B] subspectra due to the similar values of the hyperfine fields at the iron nuclei on the two sublattices of the structure. In the presence of an external magnetic field, the effective magnetiza-

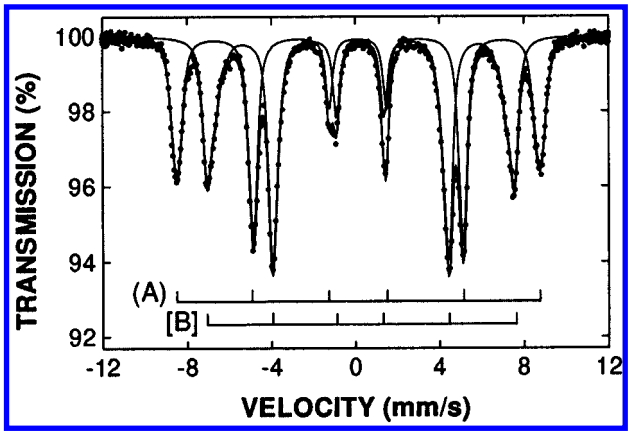

Figure 1. Mössbauer spectrum of nonactivated $MgFe_2O_4$ taken at 300 K in an applied magnetic field of 5.5 T. The field is applied perpendicular to the direction of the propagation of the Mössbauer radiation. (A) and [B] denote cation sites of tetrahedral and octahedral coordination, respectively.

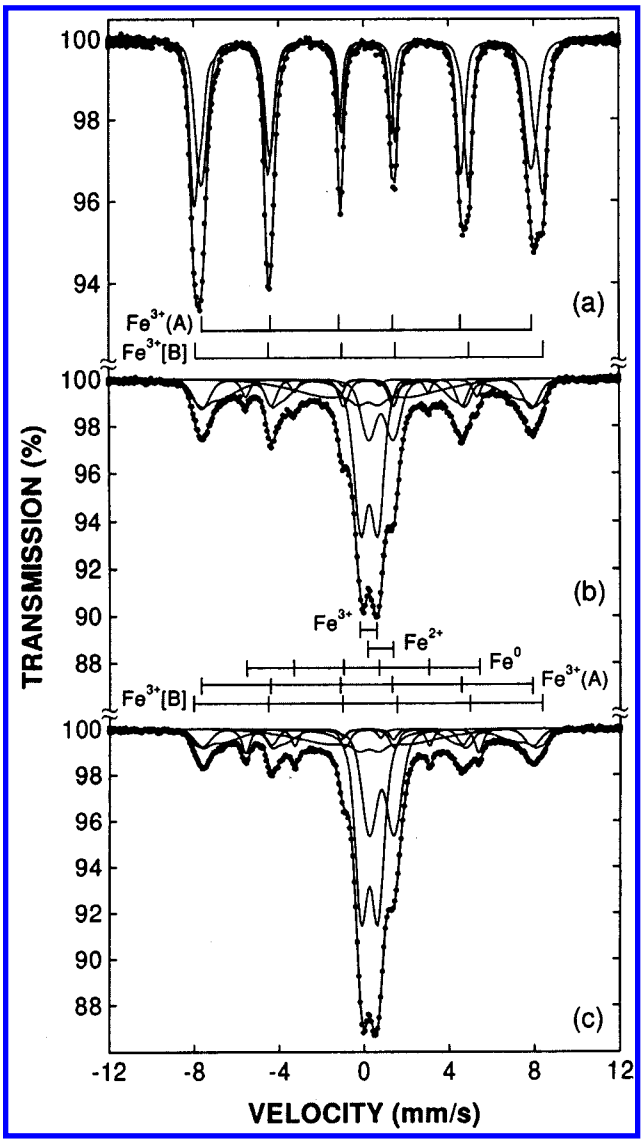

Figure 2. Room-temperature Mössbauer spectrum of nonactivated $MgFe_2O_4$ (a) and of material mechanically treated for 10 min (b) and 20 min (c) using steel milling tools.

tion of the individual particles is aligned along the field and the resulting magnetic field at the nuclei is either enhanced or decreased by the applied field.[32] In the case of nonactivated $MgFe_2O_4$ with a collinear ferrimagnetic ordering,[30] the presence of an external magnetic field results in an almost complete resolution of the overlapping patterns due to Fe^{3+} in octahedral and tetrahedral coordination (Figure 1). The degree of inversion calculated from the subspectral area ratio of the Mössbauer spectrum without and with an applied magnetic field was found to be $\lambda = 0.913(2)$ and $\lambda = 0.917(2)$, respectively; for details, see Šepelák et al.[29] The values of the hyperfine magnetic fields ($H_A = 48.16(9)$ T, $H_B = 50.01(1)$ T), of the isomer shifts ($IS_A = 0.13(3)$ mm s^{-1}, $IS_B = 0.24(8)$ mm s^{-1}), and of the degree of inversion are in agreement with previously published data[32] showing that $MgFe_2O_4$ is a partly inverse spinel.

Mechanical activation brings about significant changes in the spectra. With increasing milling time, the hyperfine magnetic sextets of the tetrahedrally and octahedrally coordinated iron cations become asymmetric toward the inside of each line, slowly collapse, and are gradually replaced by a central doublet with broad lines (Figure 2). It should be mentioned in this context that the new doublet structure in the center of the spectra is already visible after only 3 min of milling. Further milling leads to a gradual increase of its relative weight. The important observation is that the newly created central doublet is asymmetric and consist of two components that we attribute to Fe^{3+} and Fe^{2+}. These assignments are based on the isomer shifts of the subspectra: IS = 0.24(6) mm s^{-1} for Fe^{3+} and IS = 0.81(8) mm s^{-1} for the Fe^{2+} state.[33] The quadrupolar splitting of the ferrous signal component is about 1.16 mm s^{-1}, in good agreement with splittings observed in $Mg_{1-x}Fe_xO$ mixed crystals.[34,35] Here, composition-dependent splittings have been reported with maximum values of about 1.2 mm s^{-1} for $x = 0.6$. Under the assumption that the Debye−Waller factors of the iron species are identical, the $Fe^{2+}/(Fe^{3+} + Fe^{2+})$ ratio was calculated from the areas of the two doublets. It was found to increase with increasing milling time from zero for the nonactivated sample to about 0.32 and 0.4 for the sample milled for 10 and 20 min, respectively (Figure 2). The fraction of divalent iron ions relative to the total iron content amounts to about 12.8% and 21.9% for the sample milled for 10 and 20 min, respectively. The appearance of two central doublets is characteristic of the mechanical treatment of spinel ferrites by means of steel milling tools.[23,24] In the case of high-energy milling using ceramic α-Al_2O_3 vial and balls, only a single doublet due to Fe^{3+} is observed.[28−30,36,37] Recently, this observation has also been reported for milling processes using tungsten carbide (WC) balls and vials.[38−40]

To elucidate the origin of the central doublet component assigned to the Fe^{3+} ions, it should be noted that the high-energy milling of $MgFe_2O_4$ is accompanied by the reduction of the crystallite size to the nanometer range (~10 nm). It is well-known that the most striking effect of crystallite size reduction on Mössbauer spectra is due to superparamagnetic relaxation. The latter arises if crystallite sizes are so small that thermally induced energy fluctuations can overcome the anisotropy energy and change the direction of the magnetization of a particle from one easy axis to another.[41] A material can be observed as superparamagnetic in the Mössbauer spectrum if the relaxation time τ for the reversal of magnetization in a particle is smaller than the Larmor precession time τ_L of the nuclear magnetic moment in the local field.[41] In an assembly of particles with different volumes (nonuniformity of particle sizes), the experimental Mössbauer spectra will be given by the superposition of spectra with different relaxation times, since τ is sensitive to the particle volume. Consequently, the spectral components assigned to the Fe^{3+} ions (Figures 2b and 2c) can be understood to arise from ^{57}Fe in ferrite particles with relaxation times $\tau < \tau_L$ (superparamagnetic doublet) and $\tau > \tau_L$ (slowly collapsing broadened sextets due to Fe^{3+}(A) and Fe^{3+}[B]). The broad shape of the collapsing sextets provides clear evidence of a wide distribution of magnetic fields at the Fe^{3+} nuclei in disordered $MgFe_2O_4$. This is particularly true for the octahedrally coordinated ferric ions, Fe^{3+}[B], which are very sensitive to the number of their (A)-site nearest magnetic neighbors, Fe^{3+}(A).[29] The isomer shift of the superparamagnetic signal component (IS = 0.24(6) mm s^{-1}) is characteristic of octahedrally coordinated ferric ions.[33] The slightly varying splitting of this doublet (0.78(6) mm s^{-1} < QS < 0.81(7) mm s^{-1}) indicates changes in the relaxation time τ that may be due to changing particle volumes in the course of the milling process.

In addition to the intensity decrease of the initial magnetic sextets and the formation of both Fe^{3+} and Fe^{2+} doublet components, the mechanical treatment leads to the formation of a new hyperfine magnetic sextet with an isomer shift of IS = −0.11(2) mm s^{-1} and an magnetic hyperfine field of H = 33.9(9) T, see Fe^0 in Figures 2b and 2c. This magnetic field is characteristic for metallic iron, which is given by $H(\alpha\text{-Fe})$ = 33.04 T at room temperature.[42] To conclude, the Mössbauer data clearly show that high-energy milling of $MgFe_2O_4$ is accompanied by the formation of reduced phases containing Fe^{2+} and magnetically ordered metallic iron.

In addition to the well-defined spectral contributions described above, the spectra of the milled material (Figures 2b and 2c) also contain a broad structureless background. We had to introduce this "sagging" background absorption to account for unresolved magnetic relaxation processes in a qualitative way, see, e.g., ref 43. The structureless background contains about 15% of the total spectral intensity. According to the respective spectral intensity ratio, the fraction of magnetically ordered iron increases from 0% for the nonactivated sample to about 6.3% of total iron for the sample milled for 20 min. The total atomic fraction of iron contained in the reduced phases reaches a value of about 28.2% after this time of milling. These percentages, however, may represent only lower-bound values because part of the signal intensity of the reduced phases, notably that due to metallic iron, may be contained in the sagging background of the spectrum.

To determine the phase evolution of $MgFe_2O_4$ during high-energy milling in greater detail and to support the findings of Mössbauer spectroscopy, the mechanochemical reduction was also followed by X-ray powder diffraction. The XRD pattern of the nonactivated sample (Figure 3a) is characterized by the sharp crystalline peaks corresponding to $MgFe_2O_4$ (JCPDS 17-0464). During the early stages of milling, XRD merely reveals a decrease of the intensity and an associated broadening of the Bragg peaks of the spinel. This reflects the formation of the disordered state with a small crystallite size and with internal strain introduced during the mechanical treatment. With increasing milling time, qualitative changes are observed in diffraction patterns of the samples. This can be attributed to the formation of a solid solution $Mg_{1-x}Fe_xO$ which possesses the wüstite structure (JCPDS 35-1393) and of crystalline iron (JCPDS 06-0696). This observation is similar to the behavior encountered in the case of $NiFe_2O_4$ under the same milling conditions where the mechanically induced reduction led to the formation of metallic iron and of solid solution $Ni_{1-x}Fe_xO$.[24] In both mechanochemically reduced $MgFe_2O_4$ and $NiFe_2O_4$ spinels, the

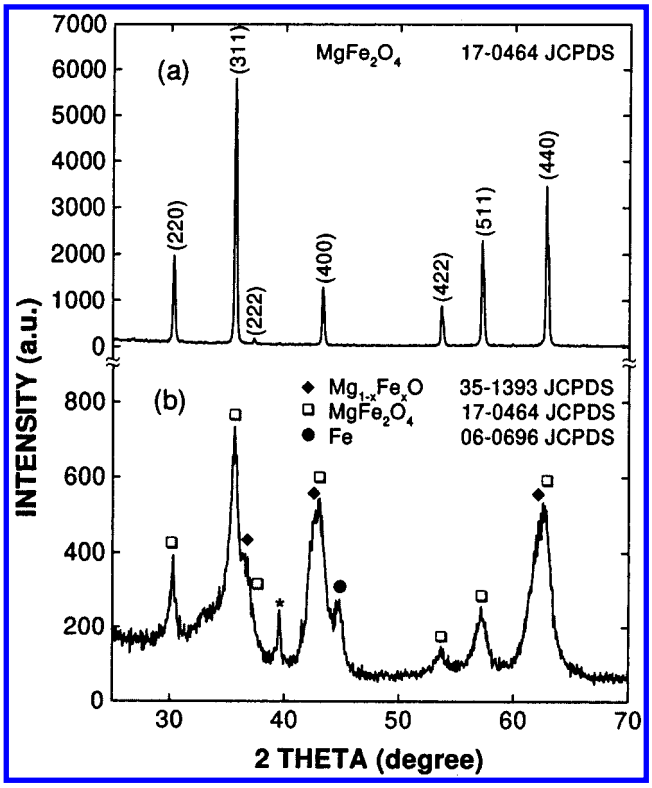

Figure 3. X-ray diffraction pattern of nonactivated $MgFe_2O_4$ (a) and of material mechanically treated for 20 min (b). Diffraction lines of $MgFe_2O_4$ are denoted by Miller indices (Figure 3a). The asterisk indicates a diffraction peak of the sample holder (Cu Kα radiation).

multiphase nature of the samples and the broadness of the diffraction lines of the nanosize milled material make it impossible to determine quantitative structural data or the exact chemical composition of the $Me_{1-x}Fe_xO$ or of a possible *Me*−Fe solid solution (*Me* = Mg or Ni).

An extensive study[44,45] of the influence of the milling conditions on the contamination of oxide (SiO_2) powders by metallic iron during high-energy milling has shown that the Fe content originating from the abrasion of the metallic milling tools increases with increasing milling time and specific mill power. However, under conditions of dry milling, abrasion exhibits a saturation behavior limiting iron wear to about 0.7 at. %, which has been attributed to an encrustation of the metallic surfaces.[44,45] Under the assumption that the material under study in the present work behaves similarly to the oxide studied in refs 44 and 45, and because pre-used balls and vials were utilized in our study, we expect that the contamination by iron abrasion is less than 1 at. %. The relatively high content (∼28.2%) of the reduced phases containing Fe^{2+} and Fe, therefore, provides evidence that the abrasion cannot be the main source of crystalline metallic iron detected in our study. Thus, on the basis of the available information on iron abrasion in dry milling experiments, we conclude that both the solid solution of $Mg_{1-x}Fe_xO$ and the ferromagnetic Fe are predominantly obtained as the result of the mechanochemical reduction of $MgFe_2O_4$. Clearly, such a mechanically induced chemical reduction in an oxygen-containing atmosphere represents an unusual and unexpected observation.

As discussed above, abrasion of the milling tools is unavoidable to some extent. Accordingly, by close inspection of the milled samples by electron microscopy and EDX analysis chromium-containing particles have been detected, which originate from the wear of the hardened steel vial and balls ($Fe_{18}Cr_8Ni$). However, a quantitative EDX analysis was not possible due to the scarcity of these observations. This is compatible with the above-mentioned information on the small extent of iron abrasion to be expected in dry high-energy milling.[44,45]

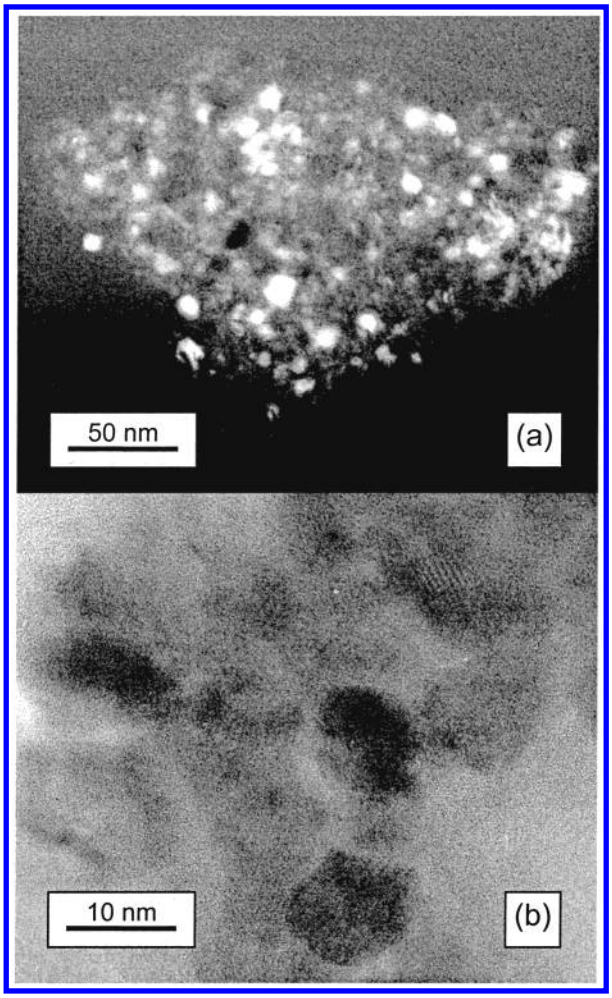

Figure 4. TEM images of the products of mechanochemical reduction of $MgFe_2O_4$.

Results from electron microscopy and particle size analysis reveal that the sizes of the powder particles of the nonactivated sample range between 10 μm to 50 μm with a specific surface of about 1.06 m^2 cm^{-3}. In the course of milling, the powder particles are subjected to continuous fragmentation. As a result, the powders become much finer and more uniform in shape. While the nonactivated $MgFe_2O_4$ consisted predominantly of individual particles, the milled samples consist of aggregates of fine particles. The specific surface area of the powders obtained was 3.2 m^2 cm^{-3}. Dark-field TEM images of the mechanochemically reduced $MgFe_2O_4$ (Figure 4a) show many bright spots indicating many small crystals. Their sizes were estimated from TEM to be about 10 nm (Figure 4b).

The spinel ferrites are known to be stable and chemically inert refractory compounds. According to the phase diagram of the Mg−Fe−O system,[46,47] $MgFe_2O_4$ can be reduced at very low oxygen activities. In a study performed at relatively low temperatures (in the range from 720 to 970 K) and using flowing hydrogen gas to ensure low oxygen activities, it has been shown that $MgFe_2O_4$ can be reduced leading to the formation of the solid solution $Mg_{1-x}Fe_xO$ and of metallic iron.[35,48] Hence, under these conditions, the same reaction products are obtained that have also been observed in the case of the mechanochemical reduction of $MgFe_2O_4$ performed in air at room temperature. Thus, the mechanically induced reduction of $MgFe_2O_4$ offers

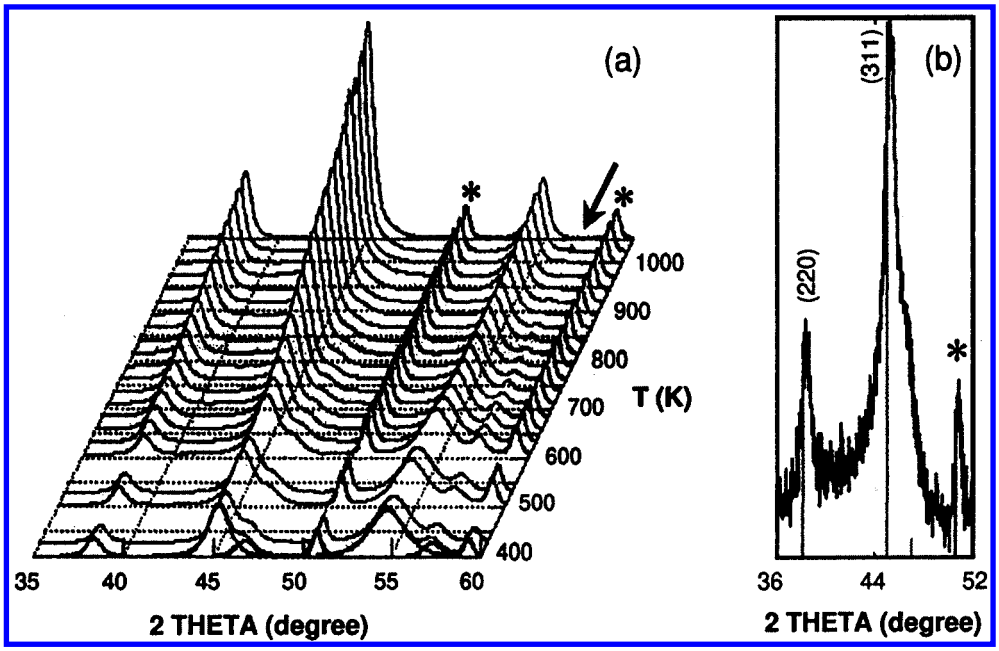

Figure 5. (a) The XRD patterns of the mechanochemically reduced $MgFe_2O_4$ taken during the thermal treatment in the high-temperature X-ray camera (Fe Kα radiation). A gradually disappearing diffraction line (due to oxidation) of metallic iron is indicated by an arrow. The sample was measured on a platinum support (*). (b) Detail of Figure 5a: the XRD pattern at 1000 K showing the asymmetry of the (311) diffraction line.

an alternative route to the conventional thermally activated solid−gas reduction process.

The products of the mechanochemical reduction reaction are metastable with respect to structural and compositional changes under temperature and environmental conditions. In situ high-temperature XRD in a flowing nitrogen atmosphere in the range from 293 to 600 K showed no change in the diffraction patterns of the milled powders. Thus, the range of thermal stability of the reduction products extends up to 600 K under these conditions. However, at temperatures above 600 K a gradual recrystallization of the nanoscale powders takes place. This is manifested by the gradual narrowing of diffraction lines and by an increase of their intensities, as shown in Figure 5a. The growth of the crystallites is accompanied by compositional changes of the reduction products. The metallic iron is gradually oxidized to Fe_3O_4 (JCPDS 19-0629) by the residual oxygen present in the nitrogen gas. This process is manifested by the gradual disappearance of the diffraction line of metallic iron and by the increase of the diffraction line intensities of the spinel phase (Figure 5a). More direct evidence for the formation of magnetite, however, is provided by Mössbauer spectroscopy. The second product of the mechanochemical reduction, the solid solution $Mg_{1-x}Fe_xO$, is relatively stable with respect to temperature. The presence of this phase in the thermally treated samples is reflected by the asymmetry of the (311) diffraction line of the spinel phase (at $2\Theta \approx 45°$) on its right-hand side (Figure 5b).

After the annealing of the multiphase mixture, the formation of magnetite and the partial oxidation of the solid magnesiowüstite solution was confirmed by Mössbauer spectroscopy. The Mössbauer spectrum of the sample milled for 20 min after annealing at 1000 K in nitrogen atmosphere (Figure 6) shows the sextets corresponding to magnetically ordered $MgFe_2O_4$ and Fe_3O_4 as well as the paramagnetic doublet characteristic of Fe^{2+} cations in the solid solution. No indication of Fe and Fe_2O_3 was observed. As expected, the superparamagnetic doublet component assigned to the Fe^{3+} ions vanished due to recrystallization and the growth of spinel ferrite particles. The disappearance of the broad, structureless absorption used to describe the "sagging" of the Mössbauer spectra (Figure 2) indicates that this spectral component is associated with the presence of small particles exhibiting magnetic relaxation phenomena (superparamagnetism and/or collective magnetic excitations). The quantitative evaluation of the Mössbauer spectra revealed that the thermal treatment of the milled samples results in a decrease of the Fe^{2+} content in the solid solution by about 5% when compared with the sample before annealing. This indicates that in addition to the complete oxidation of metallic iron, also a partial oxidation of the solid $Mg_{1-x}Fe_xO$ solution takes place during heating.

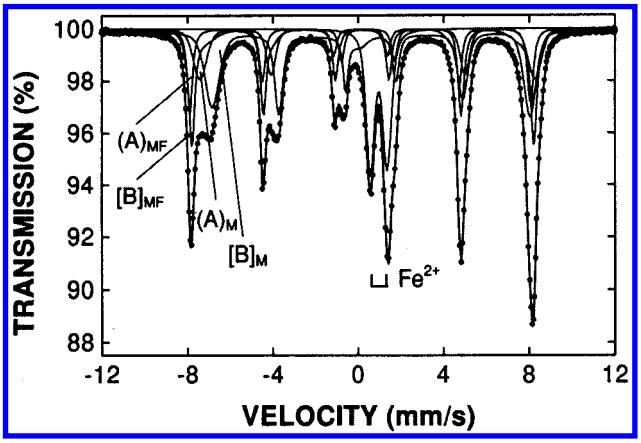

Figure 6. Mössbauer spectrum of the mechanochemically reduced $MgFe_2O_4$ after annealing at 1000 K in nitrogen atmosphere. Cation sites of tetrahedral (A) and octahedral [B] coordination in the spinels $MgFe_2O_4$ (MF) and Fe_3O_4 (M) are indicated by $(A)_{MF}$, $[B]_{MF}$, and $(A)_M$, $[B]_M$, respectively. The doublet in the center of the spectrum corresponds to ferrous ions in magnesiowüstite, $Mg_{1-x}Fe_xO$.

The information on the structural response of the mechanochemical reduction products to changes in temperature obtained by in situ XRD and Mössbauer spectroscopy was complemented by thermogravimetric measurements performed in a nitrogen atmosphere. The thermal treatment of the nonactivated sample in the range from 293 to 1000 K does not produce any mass changes. In contrast, heating the milled samples (Figure 7) leads to a mass increase due to oxidation of the reduced phases by

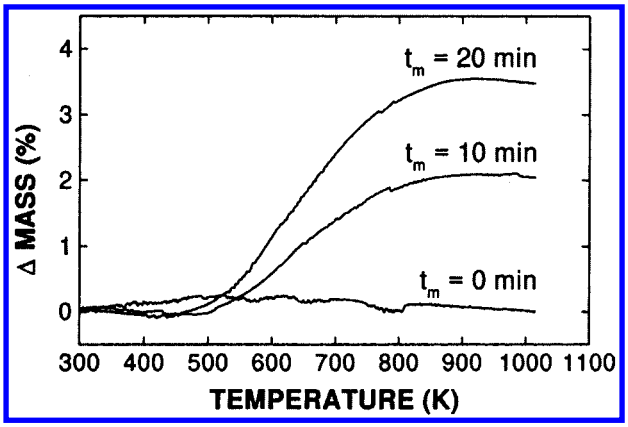

Figure 7. Thermogravimetric curves of $MgFe_2O_4$ mechanically treated for various times (t_m).

the residual oxygen present in the flowing nitrogen gas. If the atomic fraction of iron that reacts with oxygen during heating amounted to only 11.3% (6.3% Fe^0 + 5% Fe^{2+} in the solid solution), a mass increase of about 2.8% could be expected upon reoxidation of the metallic iron and partial reoxidation of the solid solution. This is in reasonable agreement with the experimental mass change of up to 3.5% observed for the milled material (Figure 7).

In view of the fact that the milling process is carried out in air, the appearance of reduced phases is a surprising experimental result. Although several mechanisms have been proposed for the reduction processes occurring during high-energy milling,[11−13,26,49] to our best knowledge, no conclusive explanation for mechanically induced redox reactions has been given yet. Kaczmarek et al.[12,49] suggested that the mechanochemical reduction process takes place at the surface of the milled oxide. According to these authors, oxygen bonds on the cleaved oxide surfaces are broken during the mechanical treatment leading to the reduction of the sample and to a release of oxygen to the vial's internal volume. In this case, the rupture of oxide surface layers and surface stress are assumed to provide the driving force for the reduction.

It has also been proposed that the oxygen partial pressure in the vial atmosphere is the critical parameter responsible for the mechanochemical reduction. Zdujic et al.[15,50] presumed that adsorption of oxygen on atomically clean surfaces created by particle fracture may cause a decrease of the oxygen partial pressure to some critical value below which the given phase becomes locally unstable and transforms to a stable one. The transformation occurs at the moment of impact by the formation of high-energy localized sites of short lifetime (sometimes called "hot spots" or "thermal spikes").

Also the role of milling tools has been considered in the context of mechanically induced chemical reduction. It has been assumed by numerous authors that the contamination originating from the abrasion of the vial and the balls is insignificant for the reduction reaction.[12,13,26,49] In contrast, Kosmac et al.[11] suggested on the basis of their experiments on milled α-Fe_2O_3 powders that contamination by Fe from the stainless steel vial and balls can cause the reduction of Fe^{3+} to a mixture of Fe^{3+} and Fe^{2+}, i.e.: $4\alpha\text{-}Fe_2O_3 + Fe \rightarrow 3Fe_3O_4$. However, the relatively small amount of iron contamination of up to 1% typical for dry high-energy milling[44,45] seems to imply that this process cannot really account for the extensive reduction observed in the present case. Thus, we conclude that an interaction between a possible iron contamination and the milled oxide is not the dominant process in the mechanochemical reduction of $MgFe_2O_4$.

Another important factor to be considered in the context of mechanochemical reaction is the mass of the balls in the high-energy milling which strongly influences the impact energies. It has been demonstrated that high-energy milling of spinel ferrites using alumina balls, whose density is lower than that of steel milling tools, does not lead to chemical reduction.[28−30,36,37] Similarly, the use of WC milling tools, which are heavier than steel ones, does not lead to chemical reduction of spinels.[38−40] In view of these results, it appears that the mass of the balls (and consequently the possible "hot spot" temperature) cannot be the dominant factor responsible for the observed mechanochemical reduction process. Taking into account this fact together with the present evidence and that obtained in the analogous system $NiFe_2O_4$,[24] it may be stated that the material of the vial and balls plays an essential role in the mechanochemical transformation of spinel ferrites. As an alternative to the above indicated views, the reduction process could be understood as result of a short-time equilibration between spinel and the encrusted metallic iron phase of the milling tools during the impact period. The oxidation of the metallic ball, however, may be kinetically hindered, leading instead to the liberation of oxygen. Impact-induced local heating and high pressures may provide further factors enhancing this reduction mechanism of the spinel. In this context, the minute quantities of abraded iron could play an initiating, catalytic role. To conclude, the identification of the factors representing the main driving force for mechanically induced redox processes, the elucidation of the microscopic mechanism(s), and the determination of rate-determining steps of mechanochemical reduction represent major challenges for fundamental research and require further efforts.

Conclusions

The changes in $MgFe_2O_4$ induced by high-energy milling in a stainless steel vial have been investigated by Mössbauer spectroscopy, X-ray diffraction, electron microscopy, and thermal analysis. In addition to the formation of nanoscale ferrite particles, the mechanical treatment results in the mechanochemical reduction of $MgFe_2O_4$ leading to the formation of a solid solution $Mg_{1-x}Fe_xO$ and of a metallic iron phase. The fraction of the reduced phases increases with increasing milling time.

Due to its local nature, Mössbauer spectroscopy has proven its exceptional ability to discriminate different valence states, magnetic states, and local coordination of iron ions in nanocrystalline mechanically treated spinel ferrites. Both these properties of local atomic and magnetic structure as well as phase analysis of nanoscale materials are especially valuable in view of the fact that diffraction techniques lose much of their resolving power in such systems.

The nanocrystalline products of the mechanochemical reduction are metastable with respect to structural and compositional changes at elevated temperatures. In a nitrogen atmosphere, the range of the thermal stability of the nanoscale product extends up to about 600 K. At temperatures above 600 K, the nanosize product gradually begins to crystallize. This is accompanied by the oxidation of the metallic iron to Fe_3O_4, while the solid solution is relatively stable chemically during the annealing.

In the context of a mechanistic analysis, we conclude that the metallic nature of the vial and of the balls plays an essential role in the mechanochemical reduction process. However, the details of this process and factors influencing it remain open and require further study. It appears that the event of mechanically induced redox reactions presents novel opportunities for the nonthermal manipulation of materials and provides a promising field for future fundamental as well as applied research.

Acknowledgment. This work was supported by the Alexander von Humboldt Foundation and Slovak Grant Agency for Science (Grant 2/7040/20). Financial assistance by the Fonds der Chemischen Industrie is gratefully acknowledged.

References and Notes

(1) For example, Schumacher, P.; Warren, P.; Cantor, B. *Metastable, Mechanically Alloyed and Nanocrystalline Materials*; Trans Tech Publications: Zürich, 2001; Boldyrev, V. V. *Reactivity of Solids: Past, Present and Future*; Blackwell Science: Oxford, 1996.

(2) Avvakumov, E. G. *Mechanical Methods of Activation of Chemical Processes*; Nauka: Novosibirsk, 1986 (in Russian).

(3) Schaffer, G. B.; McCormick, P. G. *Appl. Phys. Lett.* **1989**, *55*, 45.

(4) Takacs, L. *Nanostruct. Mater.* **1993**, *2*, 241.

(5) Basset, D.; Matteazzi, P.; Miani, F.; Le Caër, G. *Hyperfine Interactions* **1994**, *95*, 2235.

(6) Tokomitsu, K. *Solid State Ionics* **1997**, *101*−*103*, 25.

(7) Kerr, A.; Welham, N. J.; Willis, P. E. *Nanostruct. Mater.* **1999**, *11*, 233.

(8) Goya, G. F.; Rechenberg, H. R. *J. Phys.: Condens. Matter* **2000**, *12*, 10579.

(9) El-Eskandarany, M. S.; Omori, M.; Konno, T. J.; Sumiyama, K.; Hirai, T.; Suzuki, K. *Metall. Mater. Trans. A* **2001**, *32*, 157.

(10) Oleszak, D.; Krasnowski, M. *Mater. Sci. Forum* **2001**, *360*−*362*, 235.

(11) Kosmac, T.; Courtney, T. H. *J. Mater. Res.* **1992**, *7*, 1519.

(12) Kaczmarek, W. A.; Ninham, B. W. *IEEE Trans. Magn.* **1994**, *30*, 732.

(13) Campbell, S. J.; Kaczmarek, W. A.; Wang, G. M. *Nanostruct. Mater.* **1995**, *6*, 735.

(14) Jiang, J. Z.; Zhou, Y. X.; Mørup, S.; Koch, C. B. *Nanostruct. Mater.* **1996**, *7*, 401.

(15) Zdujić, M.; Jovalekic, Ć.; Karanovic, Lj.; Mitrić, M. *Mater. Sci. Eng. A* **1999**, *262*, 204.

(16) Yang, H.; McCormick, P. G. *J. Solid State Chem.* **1993,** *107*, 258.

(17) Ding, J.; Miao, W. F.; Tsuzuki, T.; McCormick, P. G.; Street, R. In *Synthesis and Processing of Nanocrystalline Powder*; Bourell, D. L., Ed.; TMS: Warrendale, 1996; p 69.

(18) Welham, N. J. *J. Alloy Compd.* **1998**, *274*, 303.

(19) Welham, N. J. *Mater. Sci. Eng. A* **1998**, *248*, 230.

(20) Takacs, L. *Mater. Lett.* **1992**, *13*, 119.

(21) Sorescu, M. *J. Mater. Sci. Lett.* **1998**, *17*, 1059.

(22) Botta, P. M.; Aglietti, E. F.; Porto López, J. M. *J. Mater. Synth. Process.* **2000**, *8*, 345.

(23) Šepelák, V.; Becker, K. D. *J. Mater. Synth. Process.* **2000**, *8*, 155.

(24) Menzel, M.; Šepelák, V.; Becker, K. D. *Solid State Ionics* **2001**, *141*−*142*, 663.

(25) Shi, Y.; Ding, J. *J. Appl. Phys.* **2001**, *90*, 4078.

(26) Goya, G. F.; Rechenberg, H. R.; Jiang, J. Z. *J. Appl. Phys.* **1998**, *84*, 1101.

(27) Willey, R. J.; Noirclerc, P.; Busca, G. *Chem. Eng. Commun.* **1993**, *123*, 1.

(28) Šepelák, V.; Schultze, D.; Krumeich, F.; Steinike, U.; Becker, K. D. *Solid State Ionics* **2001**, *141*−*142*, 677.

(29) Šepelák, V.; Baabe, D.; Litterst, F. J.; Becker, K. D. *J. Appl. Phys.* **2000**, *88*, 5884.

(30) Šepelák, V.; Baabe, D.; Litterst, F. J.; Becker, K. D. *Hyperfine Interactions* **2000**, *126*, 143.

(31) Lagarec, K.; Rancourt, D. G. *Recoil* − *Mössbauer Spectral Analysis Software for Windows, version 1.02;* Department of Physics, University of Ottawa, Ottawa, 1998.

(32) O'Neill, H. St. C.; Annersten, H.; Virgo, D. *Am. Miner.* **1992**, *77*, 725.

(33) Menil, F. *J. Phys. Chem. Solids* **1985**, *46*, 763.

(34) Becker, K. D.; Dreher, S. *Ber. Bunsen-Ges. Phys. Chem.* **1989**, *93*, 1382.

(35) Ge, X.; Li, M. S.; Shen, J. Y. *J. Solid State Chem.* **2001**, *161*, 38.

(36) Šepelák, V.; Baabe, D.; Becker, K. D. *J. Mater. Synth. Proces.* **2000**, *8*, 333.

(37) Šepelák, V.; Wissmann, S.; Becker, K. D. *J. Mater. Sci.* **1998**, *33*, 2845.

(38) Chinnasamy, C. N.; Narayanasamy, A.; Ponpandian, N.; Justin Joseyphus, R.; Jeyadevan, B.; Tohji, K.; Chattopadhyay, K. *J. Magn. Magn. Mater.* **2002**, *238*, 281.

(39) Chinnasamy, C. N.; Narayanasamy, A.; Ponpandian, N.; Chattopadhyay, K. Shinoda, K.; Jeyadevan, B.; Tohji, K.; Nakatsuka, K.; Furubayashi, T.; Nakatani, I. *Phys. Rev. B* **2001**, *63*, 184108.

(40) Chinnasamy, C. N.; Narayanasamy, A.; Ponpandian, N.; Chattopadhyay, K. *Mater. Sci. Eng. A* **2001**, *304*−*306*, 983.

(41) Mørup, S. In *Mössbauer Spectroscopy Applied to Inorganic Chemistry. Vol. 2*; Long, G. J., Ed.; Plenum: New York, 1987; p 89.

(42) Spikerman, J. J.; De Voe, J. R.; Travis, J. C. Standard Reference Materials: Standards for Moessbauer Spectroscopy, NBS Special Report 260-20 1970.

(43) Hesse, J. *Hyperfine Interactions* **1989**, *47*, 357.

(44) Tkácová, K.; Števulová, N.; Lipka, J.; Šepelák, V. *Powder Technol.* **1995**, *83*, 163.

(45) Števulová, N.; Bálintová, M.; Tkácová, K. *J. Mater. Synth. Process.* **2000**, *8*, 265.

(46) Zalazinskii, A. G.; Balakirev, V. F.; Barkhatov, V. P.; Chufarov, G. I. *Russ. J. Phys. Chem.* **1975**, *49*, 914.

(47) Paladino, A. E. *J. Am. Ceram. Soc.* **1960**, *43*, 183.

(48) Qian, Y. T.; Kershaw, R.; Dwight, K.; Wold, A. *Mater. Res. Bull.* **1983**, *18*, 543.

(49) Kaczmarek, W. A.; Onyszkiewicz, I.; Ninham, B. W. *IEEE Trans. Magn.* **1994**, *30*, 4725.

(50) Zdujic, M.; Jovalekic, C.; Karanovic, Lj.; Mitric, M.; Poleti, D.; Skala, D. *Mater. Sci. Eng. A* **1998**, *245*, 109.